Semiconductor Physics, Quantum Electronics & Optoelectronics. 2002. V. 5, N 3. P. 322-327.

PACS: 07.07.D

Effect of mechanical stress on operation of diode temperature sensors

V.L. Borblik, Yu.M. Shwarts, E.F. Venger
Institute of Semiconductor Physics, NAS of Ukraine, 45 prospect Nauki, 03028 Kyiv, Ukraine
Phone: 265-62-92, e-mail: zinovi@lab2.semicond.kiev.ua

Abstract. Effect of uniaxial elastic strain (of moderate magnitude) on operation of n^+- p-type diode temperature sensor made in silicon is considered theoretically. It is assumed that operating current and stress direction coincide with each other and with one of three main crystallographic directions [100], [110] and [111]. The cases of long and short diodes, compressive and tensile stresses are studied. It is shown that, under such conditions, two components of the piezojunction effect (namely: change in the minority carrier mobility and change in the intrinsic carrier concentration) act oppositely to each other. As a result, effect of longitudinal parasitic mechanical stress on indications of the silicon diode temperature sensors proves to be minimal in the direction of [100]-type [111]-type as it would be expected from rather than piezoresistivity of n-Si.

Keywords: diode temperature sensor, mechanical stress, piezojunction effect, silicon.

Paper received 10.04.02; accepted for publication 10.12.02.

1. Introduction

Use of small-size diodes and transistors (of the order of tens micrometers) as the temperature sensors brings up a problem of an influence on their indications of mechanical stresses which develop in the microdevices under their manufacturing and operation. Such mechanical stresses are reliably registered by up-to-date means of measurement and reach of 200 MPa and more [1,2].

Theory of the diode temperature sensors did not take into account so far these internal mechanical stresses. But the attempts were undertaken to calculate an effect of external mechanical stress on current-voltage characteristics of the diodes and transistors (piezojunction effect, or tensodiode effect). The well-known piezoresistance effect enters into the piezojunction effect as one of its components. Another its component is change in an intrinsic carrier concentration related to change in a bandgap width (under stress) of the semiconductor in which the device is made.

So, in Ref. 3 calculations of the piezojunction effect in Ge and Si (for compressive stress) have been carried on where it was supposed that light and heavy holes are characterized by the same effective mass, which did not vary with stress. Herewith, the theoretically calculated values of the deformation potentials were used. In Ref. 4, two kinds of holes have been taken into consideration and the values of the deformation potentials determined from the experiments have been used. However, calculation of the stress-induced changes in the hole energy spectrum in Ref. 4 were based on the limiting case of large strains which is not adequate to moderate mechanical stress developing in the device structures. Recently, the paper [5] has appeared which take into account the energy spectrum of silicon under stress in full detail (numerically). But this paper is restricted by one specific stress orientation in silicon transistor along <130>-direction. (We separate ourselves here completely from the papers concerned with the tensodiode effect in large-size structures where stress-induced conductivity anisotropy gives rise to lateral redistribution of injected carrier concentration and, as a consequence, substantial generation-recombination processes at the side diode surfaces [6,7].)

In this paper, we develop an analytical theory of longitudinal piezojunction effect (both in diodes and transistors) when the operating current and stress are oriented along one of three basic crystallographic directions [100], [110], and [111]. Herewith, both compressive and tensile stress is considered.

2. General relations

When using p-n diode (or emitter-base junction of transistor) as the temperature sensor, one is interested in variation of the voltage drop, U, across the p-n junction with temperature T at constant magnitude of the operating current through the device. The dominanting mechanism of current flow in the diodes made of Ge and Si (at non-cryogenic temperatures) is the diffusion of current carriers injected into the device base (see, for example, our paper [8]). Under these conditions, the change, ΔU, in the voltage drop across the p-n junction due to action of the mechanical stress σ_{ij} (of any origin) is given by

$$\Delta U = \frac{kT}{q}\ln\left[\frac{s(o)J_s(o)}{s(\sigma)J_s(\sigma)}\right], \tag{1}$$

where q is the elementary charge, k is the Boltzmann constant, s is the cross-section area of the p-n junction, J_s is the saturation current density.

Effects connected with changes in the geometric device sizes under stress are negligible in comparison with electrophysical changes; therefore

$$\Delta U = -\frac{kT}{q}\ln\left(\frac{J_s(\sigma)}{J_s(o)}\right). \tag{2}$$

In the most realistic case of infinitely high rate of nonequilibrium carrier recombination at the base edge adjoined with the metal contact (or transistor collector), the saturation current density can be written as (see, for example, Ref. 9)

$$J_s = kT\frac{n_i^2}{N_B}\frac{\mu_{minor}}{L_{minor}}\coth\left(\frac{d}{L_{minor}}\right), \tag{3}$$

where n_i is the intrinsic carrier concentration, N_B is the base doping level (for simplicity, the step-like doping profile is supposed), μ_{minor} and L_{minor} are mobility and diffusion length of the minority carriers, respectively, d is the base length. Here and further the classic statistics is assumed to be applicable.

In the diodes with long base ($d >> L_{minor}$) Eq. (2) takes the form

$$\Delta U = -\frac{kT}{q}\ln\left[\frac{n_i^2(\sigma)}{n_i^2(o)}\left(\frac{\mu_{minor}(\sigma)}{\mu_{minor}(o)}\frac{\tau(0)}{\tau(\sigma)}\right)^{1/2}\right] =$$

$$= -\frac{kT}{q}\ln\left[\frac{n_i^2(\sigma)}{n_i^2(o)}\left(\frac{\mu_{minor}(\sigma)}{\mu_{minor}(o)}\right)^{1/2}\right], \tag{4}$$

where the minority carrier lifetime, τ, is considered to not vary with the strain. But in the diodes with short base (or in transistor) where $d << L_{minor}$ Eq. (2) reduces to

$$\Delta U = -\frac{kT}{q}\ln\left[\frac{n_i^2(\sigma)}{n_i^2(o)}\frac{\mu_{minor}(\sigma)}{\mu_{minor}(o)}\right], \tag{5}$$

that is independent of the lifetime τ at all. As it will be seen below, equations (4)–(5) give rise to appreciably different final results.

It follows from Eq. (4)–(5) that the change in the temperature sensor indications due to mechanical stress, ΔU, occurs at the expense of change in both the carrier mobility and the intrinsic carrier concentration. Both effects are consequences of the semiconductor energy spectrum deformation under stress.

3. Effect of strain on the energy spectrum of electrons and holes in Ge and Si

Effect of the strain on the energy spectrum of electrons in Ge and Si consists, mainly, in the energy shift $\delta E_c = E_c - E_{co}$ of the equivalent valleys (variation of the effective masses comes into being under large enough stresses):

$$\delta E_c^{(m)} = \sum_{ij}\left[\Xi_d\delta_{ij} + \Xi_u e_i^{(m)} e_j^{(m)}\right]u_{ij}. \tag{6}$$

Here superscript m is the valley number, $\vec{e}^{(m)}$ is the unit vector directed to the center of mth valley from the origin of coordinates in the reciprocal crystal lattice, u_{ij} is the strain tensor, Ξ_d and Ξ_u are the deformation potentials of the conduction band.

If the strain is such that different valleys shift differently, then electron transfer effect takes place and electron mobility changes.

Effect of the strain on the energy spectrum of holes reduces to lifting of the degeneracy between light- and heavy-hole subbands at wave vector $\vec{k} = 0$ and deformation of the hole dispersion law [9, 10]. The shift $\delta E_v^{h,l} = E_v^{h,l} - E_{vo}^{h,l}$ of the subband edges is given by

$$\delta E_v^{l,h} = a(u_{xx} + u_{yy} + u_{zz}) \pm$$

$$\mp\sqrt{\frac{b^2}{2}\left[(u_{xx}-u_{yy})^2 + (u_{xx}-u_{zz})^2 + (u_{yy}-u_{zz})^2\right] + d^2(u_{xy}^2 + u_{xz}^2 + u_{yz}^2)}, \tag{7}$$

where a, b, and d are the deformation potentials of the valence band. The hole mobility changes at the expense of both repopulating of two upper branches of the valance band and deformation of the hole dispersion law (which is accompanied by the effective mass changes).

Simultaneous shift of the conduction band edge as well as the valence band one determines the change in the indirect band-gap width which results in the intrinsic carrier concentration change.

The strain sensor u_{ij} in the Eqs. (6)–(7) is expressed in the terms of the stress tensor σ_{kl} by means of Hook's law

$$u_{ij} = \sum_{kl} S_{ijkl}\sigma_{kl}, \tag{8}$$

where S_{ijkl} are components of the elastic compliance tensor of the 4th rank. For practical calculations, instead of the true strain tensor components, the conventional (or technical) strain components ε_{ij}, are used. They differ from u_{ij} by twice as much off-diagonal elements.

When using in Eq. (8) of pair-wise subscripts (in accordance with the scheme $xx \to 1, yy \to 2, zz \to 3, yz \to 4, zx \to 5, xy \to 6$) the tensor S_{ijkl} is replaced by the matrix $S_{\alpha\beta}$ with dimensions 6×6

$$u_\alpha = \sum_{\beta=1}^{6} S_{\alpha\beta}\sigma_\beta \ , \tag{9}$$

where, for the crystals of cubic symmetry, only 3 independent components remain [13]:

$$S_{\alpha\beta} = \begin{pmatrix} S_{11} & S_{12} & S_{12} & 0 & 0 & 0 \\ S_{12} & S_{11} & S_{12} & 0 & 0 & 0 \\ S_{12} & S_{12} & S_{11} & 0 & 0 & 0 \\ 0 & 0 & 0 & \frac{1}{4}S_{44} & 0 & 0 \\ 0 & 0 & 0 & 0 & \frac{1}{4}S_{44} & 0 \\ 0 & 0 & 0 & 0 & 0 & \frac{1}{4}S_{44} \end{pmatrix} . \tag{10}$$

4. The case of silicon n$^+$-p diode

In this case it is necessary to know the change in mobility only for electrons; as to holes it is enough to know the changes in their effective masses.

We can write the expression for equilibrium electron concentration $n(\sigma)$ under stress as follows

$$\frac{n(\sigma)}{n(0)} = \frac{\sum_{m=1}^{3} n^{(m)}(\sigma)}{\sum_{m=1}^{3} n^{(m)}(0)} =$$

$$= \frac{1}{3}\sum_{m=1}^{3}\frac{\exp[-(E_c^{(m)} - E_F)/kT]}{\exp[-(E_{c0} - E_{F0})/kT]} =$$

$$= \frac{1}{3}\exp\left(\frac{\delta E_F}{kT}\right)\sum_{m=1}^{3}\exp(-\delta E_c^{(m)}/kT) \ , \tag{11}$$

where $n^{(m)}$ is the population of the pair of valleys located on the axis of <100>–type, $\delta E_F = E_F - E_{F0}$ is the Fermi level shift under stress. Herewith, the mobility of minority electrons (considered, as usual, as majority carriers) varies in accordance with formula

$$\mu_n(\sigma) = \sum_{m=1}^{3}\frac{n^{(m)}(\sigma)}{n(0)}\mu_n^{(m)} \ , \tag{12}$$

where $\mu_n^{(m)}$ is the electron mobility along the current direction, in each of 3 pairs of equivalent valleys located on the axes of <100>-type.

The expression for equilibrium hole concentration $p(\sigma)$ we can write in such a manner

$$\frac{p(\sigma)}{p(0)} = \frac{1}{m_{h0}^{3/2} + m_{l0}^{3/2}} \times$$

$$\times \left\{ m_h^{3/2}\exp[-(\delta E_F - \delta E_v^h)/kT] + \right.$$

$$\left. + m_l^{3/2}\exp[-(\delta E_F - \delta E_v^l)/kT] \right\} \tag{13}$$

where m_l and m_h are the effective masses of light and heavy holes, respectively (m_{l0} and m_{h0} are their values in absence of deformation); population of the spin-orbit split-off subband is negligible.

For complicated bands (degenerated, anisotropic, and nonparabolic) the conception of so-called carrier concentration effective mass m_{cc} is introduced [14] which allows reducing the expression for total carrier concentration in such a band to standard one. So, rigorous calculations [15] for valence band of silicon (with taking into account all 3 subbands, their anisotropy and nonparabolicity as well as spin-orbit interaction) show that changes in partial light – and heavy-hole in spite of effective masses under stress, carrier concentration effective mass m_{cc} in the valence band of stressed silicon changes very slightly in comparison with that in non-stresses state in the range of moderate mechanical stress, i.e. stress which does not exceed appreciably 10^9 dyn/cm^2 (see Tab. 1). Therefore, we will neglect thereafter in Eq. (13) changes in the effective masses of light and heavy holes with strain. But, for comparison with rigorous calculation, we will use also the expression of the form

$$\frac{p(\sigma)}{p(0)} = \left(\frac{m_{cc}}{m_{cc0}}\right)^{3/2}\exp\left[-(\delta E_F - \delta E_v^h)/kT\right] \tag{13'}$$

with m_{cc}/m_{cc0} from Ref. 15.

Then, assuming the acceptor impurities in the device base to be ionized completely and, consequently, majority carrier (hole) concentration to be independent of mechanical stress, we can find from Eq. (13) the shift of the Fermi level with strain

$$\exp(\delta E_F/kT) = \tag{14}$$

$$\left[\left(\frac{m_{h0}}{m_v}\right)^{3/2}\exp(\delta E_v^h/kT) + \left(\frac{m_{l0}}{m_v}\right)^{3/2}\exp(\delta E_v^l/kT)\right],$$

Tab. 1. Variation of the hole concentration effective mass m_{cc} in Si with compressive stress along the [100]-direction.

Compressing stress along the [100]-axis, dyn/cm^2	$\Delta m_{cc}/m_{cc0}$	m_{cc}/m_{cc0}
0	0	1
10^7	$-2.44 \cdot 10^{-4}$	0.9998
10^8	$-2.45 \cdot 10^{-3}$	0.9976
10^9	$-2.49 \cdot 10^{-2}$	0.9751

where $m_v^{3/2} = m_{h0}^{3/2} + m_{l0}^{3/2}$. Substituting (14) into (11) we find the minority carrier concentration (for electrons in p-Si) as a function of mechanical stress

$$\frac{n_p(\sigma)}{n_p(0)} = \frac{1}{3}\left[\left(\frac{m_h}{m_v}\right)^{3/2} \exp\left(\delta E_v^h / kT\right) + \left(\frac{m_l}{m_v}\right)^{3/2} \exp\left(\delta E_v^l / kT\right)\right] \cdot \sum_{m=1}^{3} \exp(-\delta E_c^{(m)} / kT)\,, \qquad (15)$$

The same expression determines the ratio $n_i^2(\sigma)/n_i^2(0)$.

4. Numerical results

The expressions for stress-dependent electron mobility in 3 main crystallographic directions are presented in Tab. 2. The mobility anisotropy constant $K = \mu_\perp / \mu_{II}$ involved in these expressions depends slightly on dominant scattering mechanism and temperature. However, for the sake of simplicity, we put it here to be equal to ratio of transversal and longitudinal electron effective masses, i.e. $K = 0.98/0.19 \approx 5.16$. Values of the rest material parameters of silicon used in calculation are shown in Tab.3. They are borrowed from Ref. 16 devoted specially to putting them to correspondence with each other.

Shown in Fig. 1 is the ratio $n_i^2(\sigma)/n_i^2(0)$ (at $T = 300$ K) as a function of uniaxial stress for three deformation directions. The dashed curve (for [100]-orientation) corresponds to taking into account accurate changes in hole effective masses through m_{cc} in accordance with Ref. 15. Difference between accurate and approximate results is of the order of 1 %. For comparison Fig. 1 shows also the results of Ref. 4 (in the compression region) demonstrating complete nonadequacy of the approach used there for the moderate stress range.

Effect of the mechanical stress on electron mobility is presented by Fig. 2. As seen from the comparison of Figs

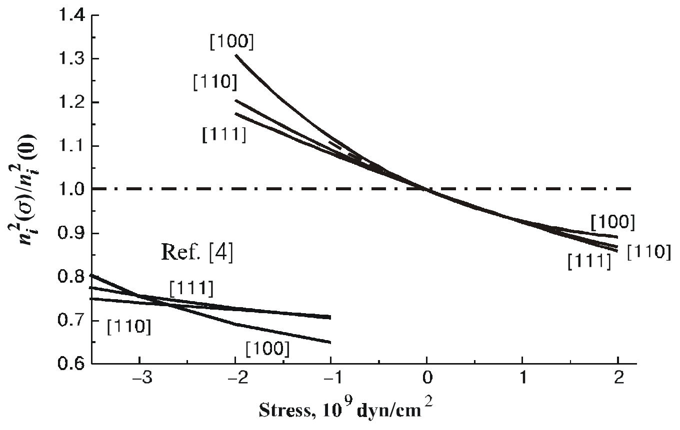

Fig. 1. Dependence of the square of the intrinsic carrier concentration on mechanical stress in three basic crystallographic directions; the dashed curve corresponds to accurate taking into account (for [100]-direction) change in common hole effective mass (see text).

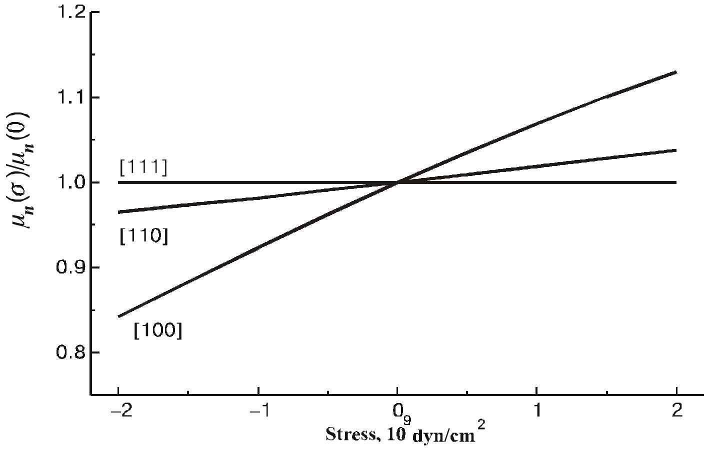

Fig. 2. Dependence of normalized electron mobility on mechanical stress in three basic crystallographic directions.

Tab. 2. The stress tensors and corresponding expressions for normalized electron mobility for three basic stress orientations.

Uniaxial stress orientation	σ_{ii}	$\mu_n(\sigma)/\mu_n(0)$	β
[100]	$\sigma\begin{pmatrix}100\\000\\000\end{pmatrix}$	$\frac{3}{2K+1}\frac{1+2Ke^{\beta\sigma}}{1+2e^{\beta\sigma}}$	$\frac{\Xi_u(S_{11}-S_{12})}{kT}$
[110]	$\frac{\sigma}{2}\begin{pmatrix}110\\110\\000\end{pmatrix}$	$\frac{3}{2K+1}\frac{1+K+Ke^{\beta\sigma}}{2+e^{\beta\sigma}}$	$\frac{\Xi_u(S_{11}-S_{12})}{2kT}$
[111]	$\frac{\sigma}{3}\begin{pmatrix}111\\111\\111\end{pmatrix}$	1	–

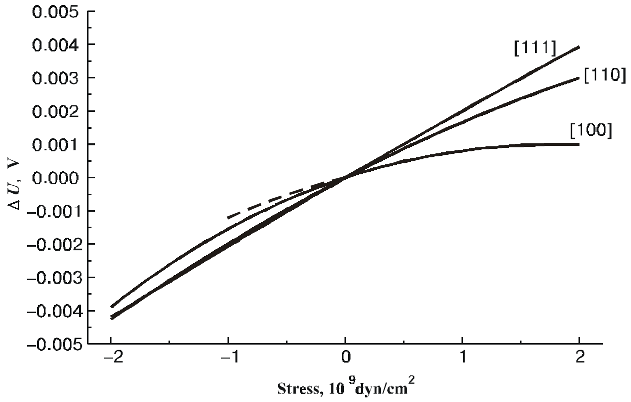

Fig. 3. Indication changes of the diode thermometer with long base versus mechanical stress; the dashed curve corresponds to accurate taking into account (for [100]-direction) change in common hole effective mass.

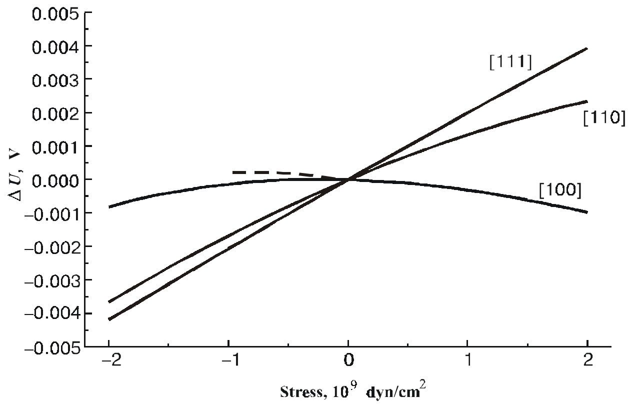

Fig. 4. Indication changes of the diode thermometer with short base (or transistor thermometer) versus mechanical stress; the dashed curve is the same as in Fig. 3.

Tab. 3. Silicon parameters used in calculations.

Parameter	Value
Ξ_d, eV	1,1
Ξ_u, eV	10,5
a, eV	2,1
b, eV	–2,33
d, eV	–4,75
$\Xi d + 1/3\,\Xi_u - $ a, eV	2,5
S_{11}, 10^{-12} cm^2/dyn	0,768
S_{12}, 10^{-12} cm^2/dyn	–0,214
S_{44}, 10^{-12} cm^2/dyn	1,26

1 and 2, piezoresistance effect (for minority carrier) and changes in the intrinsic carrier concentration act oppositely to each other: where one increases there other decreases. As a result, the diode thermometer indications change in the most strong manner in the case of the deformation action along the [111]-direction in which the electron mobility (at assumed here moderate mechanical loads) does not change (see Fig. 3 for the long-base diode and Fig. 4 – for the short-base diode, or transistor). In another deformation orientations a partial compensation of two effects takes place. In particularly, this fact manifests itself in the most bright manner in the case of short-base diode under deformation along the [100]-axes: ΔU versus stress dependence takes the form of the curve with maximum and, therefore, is characterized by small absolute values of ΔU.

5. Conclusion

Thus, it is the longitudinal parasitic deformation of the silicon n$^+$-p diode in <100>-type direction (but not <111>-type as it would be expected) that has a minimal effect on the diode temperature sensor indications. In another deformation directions studied here the error ΔU varies monotonically with stress from compression to tension and reaches (at $/\sigma/ \sim 10^9$ dyn/cm^2 = 100 MPa) 2 milivolts which is approximately equivalent to 1 K.

Though this shift can be taken into account under the device calibration, it is yet undesirable because in time, due to this correction drift, the calibration can violate.

References

1. I. De Wolf, Micro-Raman spectroscopy to study local mechanical stress is silicon integrated circuits // Semicond. Sci. Technol. **11** (2), pp. 139-154 (1996).
2. A. Szekeres and P. Danesh, Mechanical stress in SiO_2/Si structures formed by thermal oxidation of amorphous and crystalline silicon // Semicond. Sci. Technol. **11** (8), pp. 1225-1230 (1996).
3. J.J. Wortman, J.R. Hauser and R.M. Burger, Effect of mechanical stress on p-n junction device characteristics // J. Appl. Phys. **35** (7), pp. 2122-2131 (1964).
4. Y. Kanda, Effect of stress on germanium and silicon p-n junction // Japan. J. Appl. Phys. **6** (4), pp. 475-486 (1967).
5. J. F. Creemer and P.J. French, The piezojunction effect in bipolar transistors at moderate stress level: a theoretical and experimental study // Sensors and Actuators A**82** (1-3), pp. 181-185 (2000).
6. Z.S. Gribnikov, G. I. Lomova and V.A. Romanov, Injection of current carriers in anizotropic semiconductor plates and the magnetodiode effect // Phys. Stat. Sol. **28** (2), pp. 815-825 (1968).
7. Z.S. Gribnikov, I.P. Zhadko, V.A. Romanov and B.K. Serdega, Tensodiode effect under bending of long semiconductor diode-plates // Ukrainskii Fizicheskii Zhurnal, **15** (2), pp. 300-314 (1970) (in Russian).
8. Yu. M. Shwarts, V.L. Borblik, N.R. Kulish, E.F. Venger and V.N. Sokolov, Limiting characteristics of diode temperature sensors // Sensors and Actuators A **86** (3), pp. 197-205 (2000).
9. N.A. Penin, Effect of recombination velocity at nonrectifying electrode on frequency properties of p-n junction for the case of small alternating voltages // Radiotekhnika i Electronika, **2** (8), pp. 1053-1061 (1957) (in Russian).
10. C. Herring and E. Vogt, Transport and deformation-potential theory for many-valley semiconductors with anisotropic scattering // Phys. Rev. **101** (3), pp. 944-961 (1956).
11. G.E. Pikus and G.L. Bir, Effect of deformation on the hole energy spectrum of germanium and silicon // Sov. Phys. - Solid State, **1** , pp. 1502-1517 (1960).
12. G.L. Bir and G.E. Pikus, Symmetry and stain-induced effects in semiconductors, Wiley, New York (1974).
13. J.C. Hensel and G. Feher, Cyclotron resonance experiments in uniaxially stressed silicon: valence band inverse mass parameters and deformation potentials // Phys. Rev. **129** (1), pp. 1041-1062 (1963).
14. F.L. Madarasz, J. E. Land and P.M. Hemeger, Effective masses for non-parabolic bands in p-type silicon // J. Appl. Phys. **52** (7), pp. 4646-4648 (1981).
15. T. Manku and A. Nathan, Valence-band structure for strained group-IV semiconductors // J. Appl. Phys. **73** (3), pp. 1205-1213 (1993).
16. M.V. Fischetti and S.E. Laux, Band structure, deformation potentials and carrier mobility in strained Si, Ge, and SiGe alloys // J. Appl. Phys. **80** (4), pp. 2234-2252 (1996).